SPE 102781

Wellbore Stability Study for the SAFOD Borehole through the San Andreas Fault

Pijush Paul, SPE, Mark Zoback, SPE, Stanford University

This paper was prepared for presentation at the 2006 SPE Annual Technical Conference and Exhibition held in San Antonio, Texas, U.S.A., 24–27 September 2006.

Abstract

This paper presents a wellbore stability study of the SAFOD (San Andreas Fault Observatory at Depth) research borehole located near Parkfield, central California. In the summer of 2005, the SAFOD borehole was successfully drilled through the active trace of San Andreas Fault (SAF) in an area characterized by fault creep and frequent microearthquakes. In this study we report how the analysis of wellbore failures in the upper part of the hole, geophysical logs and a model for stress gradients in the vicinity of the fault were used to estimate the mud weights required to successfully drill through the fault. As logging-while-drilling (LWD) acoustic caliper data and real-time hole volume calculations both showed that relatively little failure occurred while drilling through the SAF, the predicted mud weight was successful in drilling a stable borehole. However, a six-arm caliper log run after drilling was completed indicates that there was deterioration of the borehole with time, which appears to be caused by fluid penetration around the borehole. The LWD resistivity measurements show that essentially no fluid penetration occurred as the hole was being drilled. Because of this, the mud weight used was capable of maintaining a stable wellbore. However, the resistivity data obtained after drilling shows appreciable fluid penetration with time, thus negating the effectiveness of the mud weight and leading to time-dependent wellbore failure. Using Finite Element Modeling (FEM) we show that mud penetration into the fractured medium around the borehole causes failure with time.

Introduction

Drilling perturbs the stress state around a well and wellbore stability problems can occur when the near-wellbore stresses substantially exceed the strength of the rock. Excessive instability around a wellbore can be suppressed by choosing an optimally stable borehole orientation and sufficiently high mud weight. Some wellbore wall failures such as key seating, usually do not cause instability in the borehole but can exacerbate failure in an already unstable borehole.

As described below, drilling through the SAF in the SAFOD project was done in various phases. In this paper, we discuss an analysis of wellbore failures after the first phase of drilling in order to predict the mud weight required to successfully drill through the SAF during the second phase of the project. The main challenges during the SAFOD drilling were the unknown stress field and rock strength along the planned drilling trajectory. Hence, to estimate the mud weight to be used for drilling the San Andreas Fault zone, we first calibrated a theoretical stress model[1] for the SAF with the observed borehole failures and minifrac test data during the first phase of drilling. Then, we estimated and calibrated a uniaxial compressive strength (UCS) profile for the rocks encountered by modeling the severity of borehole failures, allowing for a wide range of expected rock strengths due to the possibility of extensive damage of the rocks due to earthquakes on the San Andreas fault.

As will be shown, LWD caliper data during the second phase of drilling shows successful drilling through the SAF using the estimated mud weights inferred from the geomechanical model. However, wireline calipers were enlarged at the top section of the borehole indicating severe failure with time. We use FEM modeling to show the borehole failure with time. Block theory[2,3], used for the stability of underground openings, suggests that only the removable blocks of the top section fail due to gravity but the lower section remains in gauge despite having removable blocks. This explains why the time dependent enlargement of the SAFOD borehole is restricted to only the top section of the hole.

The San Andreas Fault and the SAFOD location

The San Andreas Fault (SAF) is a transform fault that is the principal zone of deformation accommodating relative motion between the Pacific and North American Plates. The Pacific Plate moves ~48mm/yr to the northwest relative to the North American Plate. The SAFOD well is located near Parkfield, CA, roughly halfway between San Francisco and Los Angeles (**Fig. 1**). The drillsite is on a segment of the San Andreas Fault that moves through a combination of aseismic creep and repeating microearthquakes. In the vicinity of the drillsite, nearly all the slip on the fault is aseismic, with the many small earthquakes contributing little to the overall slip rate.

The SAFOD borehole is located on the west side of the San Andreas Fault where the bedrock was expected to be mostly granitic at depth, with and rocks associated with the

Franciscan Formation expected on the eastern side of the fault. In fact, the geology turned out to be more complicated than this with arkosic sandstone and conglomerates (derived from the granites) on the west side of the fault and most of formations encountered on the east side of the San Andreas consisting of the Great Valley formation[4]. The fault zone itself is presumed to consist of crushed breccias and fault gouges. The width of the zone of intense deformation at depth (i.e., the SAF zone itself), as well as that of the damage zone surrounding the fault, were unknown prior to drilling

The SAFOD drilling plan

The SAFOD project was carried out in multiple phases. As shown in **Fig. 2**, a vertical Pilot Hole, located 1.8km to the southwest of the SAF, was drilled in 2002 and encountered granitic rock at ~850m as predicted by geophysical data. The design of the main SAFOD borehole was to drill vertically at the same drillsite as the Pilot Hole to a depth of ~1.5km and then drill a deviated hole through the fault zone in the vicinity of microearthquakes (M ~2 and smaller) located by Thurber et al.(2004). In the summer of 2004, Phase-1 was completed to a measured depth (MD) of 3048m. After the Phase-1, the borehole was logged, cased and cemented, and a seismic study was carried out in the borehole to improve knowledge of subsurface velocities and the location of the target microearthquakes. Utilizing this information, Phase-2 was carried out during the summer of 2005. The study reported here describes how we used data from Phase-1 to predict an optimum mud weight for drilling through the SAF in Phase-2. Conventional rotary drilling was used for both Phases 1 and 2 and extensive cuttings samples were collected, sophisticated real-time gas sampling was done in real-time and comprehensive geophysical logging was carried out. Having obtained this information through the SAF zone, multilateral core holes were drilled through the fault zone in summer of 2007 (Phase-3).

The vertical section of the Phase-1 borehole was mostly drilled with a 17-1/2" bit and cased with 13-3/8" casing. The deviated interval of the well (from 1.5km to 3km, MD) was drilled with a 12-1/4" bit and completed with 9-5/8"casing. The 54° deviation of the hole was achieved with a build rate of 2.5° per 30 meters. Phase-2 was drilled from 3.05km (MD) to 3.8km (MD) with an 8-1/2" bit and completed with 7" casing.[5]

Borehole stability and lithofacies for Phase 1

As interpreted from well-log analysis, three major lithofacies are intersected by the SAFOD well during Phase-1.[4] As shown in **Fig. 3**, the first 800m mostly consists of weathered Tertiary sediments. This is followed by fractured granite and granodiorite to a depth of 1926m (MD). Below that sedimentary rocks (interpreted to be made up of arkosic sandstone with interbedded shale and conglomerate) were encountered down to 3048m. These sedimentary rocks were not predicted by geological or geophysical models prior to drilling. Phase 1 borehole resistivity image logs (FMI[6]) indicate numerous natural fractures and faults throughout the entire interval drilled, as well as bedding in the sedimentary section. In conjunction with the other geophysical logs and cuttings analysis, a number of faults and brecciated zones were identified.

In general, there were relatively few problems during Phase-1 drilling even in the fault zones, although a number of trips were needed to wash and ream the hole at several depths. In **Fig. 4**, maximum and minimum diameters calculated from either the density caliper and FMI dual caliper log are presented to show the overall condition of the hole. The hole size in the sedimentary zone above 850m (that was logged only from 650-850m) is enlarged on all sides of the borehole. There is a slight improvement in hole condition in the upper, weathered granite (850-1000m), but most of the granite/granodiorite section is generally in gauge. The granodiorite section from 1440m to 1920m shows only a slight enlargement of the borehole diameter. In the fault zone at the granite/sediment contact at 1920m, we observe significant hole enlargements, again on all sides of the hole. Significant hole enlargements are also seen in the sedimentary section below 1926m, especially at some depth intervals. Better hole conditions are observed in the sandstone interval starting at 2682m.

At depths below 1440m, a detailed analysis of the caliper data reveals the orientation of borehole elongations that are ~10° anticlockwise from the top and bottom of the hole (**Fig. 4**). The fact that the borehole enlargements are close to the top and bottom of the hole suggests that they might be caused by key seating. This is discussed in more detail below.

Stress analysis

The San Andreas Fault (SAF) has been described as having low frictional strength because many in situ stress measurements show a high angle between the direction of the maximum horizontal principal stress (S_{Hmax}) and the strike of the fault[7-11] as well as the absence of frictionally-generated heat[12-13]. We developed a preliminary stress distribution model for the well trajectory based on a geodynamic model of Chery et al. (**Fig. 5**) that proposes that the SAF has a very low intrinsic friction coefficient ~0.1.[1] The possibility that the fault is characterized by anomalously high pore pressure[14], would, in effect produce very similar results but no evidence for high pore pressure was found during drilling[15]. The Chery et al. model divides the region into a near field (NF, within ~5 km of the fault) and the core of the fault zone (FZ) itself. The model predicts how stress magnitudes and the orientation of S_{Hmax} vary with depth and distance to the fault. This model predicts that the shear stress on planes parallel to the fault zone is very low and varies strongly with both distance to the fault and depth.

Close to the San Andreas fault (in the NF), Chery et al.[1] proposed that the minimum principal stress (S_3) is close to the vertical stress (S_v). The maximum principal stress (S_1), which is equivalent to S_{Hmax} is about two times the vertical stress. This stress state implies a strike-slip/reverse faulting regime[16] with magnitudes consistent with Coulomb faulting theory for laboratory-determined coefficients of friction and hydrostatic pore pressure[17]. In the model, the maximum horizontal principal stress, S_{Hmax}, is oriented N30°E, which is at high angle to the SAF. The minimum and maximum principal stresses are in a vertical plane almost perpendicular to the SAF and cause reverse faulting on faults striking parallel to the

SAF. However, the calculated normal stress acting on the fault zone (FZ) is close to S_{Hmax}. This stress state is essentially identical to that measured in the SAFOD pilot hole to 2 km depth[10]. Within the fault zone, the Chery et al. model predicts that all three principal stresses are nearly equal and close to twice the lithostatic stress, S_v, (*i.e.*, $S_1 \approx S_2 \approx S_3 \approx 2*S_v$). A theoretical model by Rice also supports this dramatic change in the value of S_3 from the near field to fault zone.[13]

For this study we obtained the lithostatic stress from density logs and other densities derived from gravity models in the drillsite area. The Chery et al. model[1] was then used to estimate principal stresses in the near field and fault zone from the lithostatic stress gradient. We used linear interpolation to define the distribution of the stress between the near field and fault zone and assumed a 300m thick fault zone that is symmetric about the surface trace of the fault. Stress and pore pressure models in the well trajectory plane are shown in **Fig. 6**. To be consistent with the observations made in the pilot hole[10], the azimuth of S_{Hmax} varies with depth. The high value for S_3 predicted by the Chery et al. model was supported by a minifrac test done at MD 3028.5m (the bottom of the casing set after completion of Phase-1 at a MD of 3000m) that was carried out at the onset of Phase-2 operations. The minifrac test was carried out in an openhole interval with highly fractured rock. However, at the maximum obtainable pressure of the used fracturing equipment (~10 MPa above the vertical stress), it was not possible to extend a hydraulic-fracture, implying that the effective minimum principal stress was appreciably above the vertical stress in the tested interval.

The Chery et al. study[1] was carried out after the Pilot Hole was drilled but before Phase-1 drilling. Three observations obtained during Phase-1 led us to slightly revise the preliminary stress model shown in **Fig. 6**. First, analysis of breakouts and drilling-induced tensile fractures and dipole sonic logs in the Phase-1 borehole indicates a maximum horizontal stress orientation of N35°E[4], which was ~5°E from that in the preliminary stress model[1]. Second, as a result of modifying the velocity model in the vicinity of the San Andreas, there was shift in the microearthquake locations to the SW. The result of this is that when Phase-1 drilling was completed, it was clear that the bottom of the hole was within 200m of the active fault zone. Third, the minifrac measurement noted above that shows extraordinarily high values of S_3 at the bottom of the Phase-1, independently confirming the fact that the active fault is close to the end of Phase-1 drilling and to the SW of the surface trace.

To constrain stress magnitudes in the arkosic rocks drilled during Phase-1, we modeled the observed borehole failures. **Fig. 7** is a wellbore stability analysis for wells of any orientation at a true vertical depth of 2220m using the methodology described by Peska and Zoback[18]. Radial distance from the center of each figure represents well deviation at a given azimuth. The figure on the left shows the orientation of a breakout (if it were to form) in a "looking down the hole" coordinate system. The figure on the right shows the magnitude of rock strength required to prevent failures larger then 60 degrees. The black arrows show the orientation of S_{Hmax}. The azimuth and orientation of the SAFOD borehole is shown in each figure. Note that the stress model used (S_1 ~101 MPa, S_2 ~91 MPa, S_3 ~50 MPa, and Azimuth of S_1 ~N35°E) predicts a breakout orientation that is 10° degrees counter clockwise from the top and bottom of the hole, exactly the same as what was observed in the caliper data (**Fig. 4**). This exercise shows, therefore, that the observed hole enlargements are stress-induced wellbore breakouts, not key seats although key seating may exacerbate the depth of the failure zones away from the borehole wall. Although this modified stress model now can be used to constrain in situ rock strength[19] in the Phase-1 wellbore in the context of the observed failures (**Fig. 4**), in the next section we first utilize geophysical logs to constrain rock strength.

UCS modeling

In cases such as this where no laboratory rock strength measurements are available, we estimate rock strength by calibrating a best fit rock strength model to the nature and severity of borehole failures. For the granite and granodiorite section between 853-1926m, we used a rock strength model (Eq. 1) of the type proposed by Annor and Jackson[20] which uses P-wave velocity measured from sonic logs to calculate rock strength. This deterministic model was later calibrated for the granite around the SAFOD well by Hickman and Zoback[10] using Pilot Hole data.

$$UCS = 129 + 0.0145 V_p \,, \tag{1}$$

where UCS is in MPa and V_p is in m/s.

To deal with the uncertainty in rock strength in the diverse sedimentary rocks that were drilled, we compared observed borehole failures with those predicted using several rock strength models[21]. These rock strength models represent a range of sedimentary environments having different values of porosity, cementation factor, clay percentage, and rock strength. We start with a coarse grained sandstone/ conglomerates (Eq. 2) proposed by Moos and Zoback[22]

$$UCS = 1.745 \times 10^{-9} \rho V_p^2 - 21, \tag{2}$$

where UCS is in MPa, ρ is in kg/m^3, and V_p is in m/s.

We found, however, that the above described sedimentary strength model tended to overestimate the rock strength (for estimated of stress magnitudes). We believe that the rock is actually weaker than predicted by Eq. 2 because of pre-existing damage and micro-cracks in the rock[23-26]. Variations of sonic velocity are incapable of completely predicting the zones of increased wellbore failures nor do density measurements indicate increased porosity associated with faults and fractures in those rocks. Resistivity images and other logs also show no increase of porosity in the failed zone. In this context, we argue that the rock weakness is caused at least in part by damage to the rock associated with discrete fractures and faults such that the overall porosity and bulk properties are relatively unchanged.

To incorporate the effect of damage on the rock strength, we use an empirical criterion proposed by Hoek and Brown[24] shown in Eq. 3. It suggests that strength of a rock mass depends on the scale of the damage. A heavily jointed rock mass behaves like an intact rock at fine scale but at larger scale behaves like an isotropic assemblage of interlocking

angular particles. Hence, the rock mass will be much weaker at large scale than fine scale.

Uniaxial compressive strength of a jointed rock mass, UCS_f, is related to uniaxial compressive strength of the intact rock, UCS, by Eq. 3.

$$UCS_f = \sqrt{s(UCS)^2} \quad (3)$$

The parameter 's' in Eq. 3 depends on interparticle tensile strength and the degree of particle interlocking. For an intact rock material s=1.0, for a damaged rock 0<s<1, and for a completely disaggregated rock, s=0. In other words, 's' decreases as the degree of fracturing of the rock mass increases because of the greater degree of freedom available to individual pieces of rock material. Laboratory tests on jointed samples of andesite and granite suggest a minimum value as low as 0.0002 for's'.[27-29] Around the SAFOD borehole, fractures are oriented in all directions so they do not introduce any intrinsic anisotropy in the rock[4].

To determine the value of compressive strength of the jointed rock using Eq. 3, we have used the UCS of intact rock calculated from Eqs. 1 and 2 using an empirical approach to estimate the value of 's' with the dual caliper measurements. To get an initial approximate value of 's', we will assume that if both calipers show that the entire hole is enlarged, we will assume that the breakout has grown into a washout with the entire circumference of the hole failing. As explained by Zoback[17], this implies an initial width ≥90°. If one caliper pairs shows large enlargement but the other shows an in gauge hole, then we assume a breakout width <90°. If both calipers are in gauge, we assume that the hole has not failed.

In **Fig. 8** we show the predicted width of breakouts in the SAFOD Phase-1 borehole using the stress model defined above for constant rock strengths that vary between 20 and 90 MPa. For rock strengths of 90 MPa no wellbore failure is seen. When rock strength is ~80 MPa, only a small amount of failure is observed in the interval 1500-1800m. Conversely, when strength is as low as 50 MPa, the prediction would be that the entire well below 1300m would be washed out. One can see, therefore, that realistic rock strengths would appear to be approximately 60-70 MPa for the assumed stress state. This enable us to estimate a value of 's' that "corrects" the log-derived strength to values consistent with those estimated from the wellbore failures. For the Tertiary section, we found s~1 because rock strength predicted by geophysical logs is low enough to model the failure observed during Phase-1 drilling. In granite/granodiorite section, we found s~1, indicating a strong rock whose strength is relatively unaffected by the fractures and faults within it. In the sedimentary section below 1926m, we found s~0.85, which predicts the degree of failure consistent with the observed amount of borehole failure.

Modeling of Phase 1 borehole failures

To evaluate how well the technique described above predicts the degree of wellbore failure observed we compare the predicted failure width with the actual wellbore failures from the maximum and minimum calipers. We define the breakout width from observed calipers by assuming breakout width less than 90°, if one caliper is in gauge and the other is enlarged. **Fig. 9** shows the minimum and maximum caliper data (column 1), the predicted strength profile (column 3) and the theoretical breakout width for s =1 (intact rock), 0.85 (~8% weaker than intact rock) and 0.7 (~16% weaker than intact rock) in the sedimentary section below 1920m and s=1 for sections above 1926m (columns 4, 5, 6). Overall, we see a very good correlation for s~0.85 in the section below 1926m. The model predicts the observed washouts in the Tertiary sediments at shallow depth. In the granite and granodiorite interval above 1926m, the borehole was observed to be generally stable which as predicted by the model. In the sandstone section interval below 1926m, the breakouts are mostly predicted to be 90° to 120° in width, which generally matches with the caliper logs fairly well although there are some intervals where there is both a predicted and observed greater amount of failure.

Based on the analysis above, the mud weight used during drilling the deeper sedimentary section in Phase-1 (~10ppg) was about 1ppg less than that which would have resulted in significantly less hole enlargement (**Fig. 10**). While a modest improvement in wellbore stability would have been achieved with an increase in mud weight of 0.5ppg, an increase of 1ppg would have resulted in significant improvements.

Mud weight prediction for Phase 2

Using the analysis presented above, we estimated the mud weight that should be used during Phase-2 drilling in four steps. First, we extrapolated the stress model down to the total depth along the proposed well trajectory. **Fig. 11** shows the modified stress models for S_2 and S_3 based on the observations made during Phase-1. Models for S_1 and P_P (both within and outside the fault zone) remain the same as that described by Chery et al.[1] Both a minifrac test done at the end of Phase-1 at MD of 3028m, (where $S_3>S_v+10MPa$). Two other minifracs tests were done, one in the vertical section of the well at MD of ~1470m and one at the bottom of hole at 4000m MD. Both indicate that the stress profile is a *classical* reverse/strike slip fault state[10] outside the fault zone as used in the Chery et. al.'s model[1]. We also assumed that the within the fault zone, stresses follow the Chery et. al. model[1]. Then we used breakout analysis (**Fig. 7**) in between the two minifrac test intervals outside the fault zone to modify the stress profile from the preliminary model. The modified values for S_2 and S_3 (**Fig. 11**) show increased values of both stresses over a broad region in compare to the preliminary model. In the second step, we extrapolated rock strength along the well trajectory. To estimate the intact rock strength using Eq. 2, we used the P-wave velocity data for the rocks to be drilled using a three dimensional seismic tomography model[30]. We observed in Phase-1 that an average bulk density of 2.68 g/cm^3 characterized the sedimentary rocks. This value was used for Phase-2. To convert intact rock strength to in situ rock strength (incorporating damage to the rocks with varying intensity), we consider a wide range for the factor 's' in Eq. 3, that goes from 0.5 to 1.0. In other words we assumed the rock strength was either unaffected by damage (s=1) or reduced by approximately 30% (s=0.5). Recall that there was only a 8% decrease (s=0.85) in the sedimentary rocks drilled in Phase-1.

The third step of the analysis was to calculate the mud weight required to drill Phase-2 utilizing a range of 's' values.

Fig. 12 show the predicted mud weight to prevent borehole failures greater than 60° breakout width. In fact, this assumption is quite conservative as many wells are drilled successfully with breakouts widths that exceed 60°. For the mean case (s~0.74), the minimum mud weight required to prevent 60° breakout is ~11.7 ppg in the fault zone and ~10.8-11.4 ppg in zones outside the fault zone. For weaker rocks (s~0.5), the required mud weights are ~12.3 ppg for the fault zone and ~11.1-12.1 ppg above and below the fault, respectively.

The fourth step of our study was to do a quantitative risk analysis (QRA) to formally incorporate the uncertainties in the extrapolated stress and rock strength values. In this way we could estimate the importance of these parameters for the prediction of minimum mud weight values.

Quantitative Risk Analysis to drill a stable borehole through the SAF

QRA allows us to incorporate uncertainty in the most expected value of the various parameters used in this study to give the probability of success using a particular mud weight.[31-32] Analysis will be done for a maximum breakout width of 60°. We allow for 10% uncertainty in stress magnitudes, a range of azimuths of the maximum horizontal stress between N30°E and N50°E, and a variation of rock strengths that corresponds to values of s ranging from 0.5 to 1.0. The QRA analysis shows in **Fig. 13a** that for a mud weight of ~11.8 ppg there is a 50% chance of success (the breakout width not exceeding 60°) in drilling through the SAF (~3300m MD). For a mud weight of 12.3 ppg there is a 90% chance of success. In **Fig. 13b** we see that rock strength (UCS) defines the uncertainty range of the estimated mud weight to drill a stable borehole with 60° breakout width. Hence, it is the most important parameter needed to drill a stable borehole through the fault zone. Hence, even with a mud weight of ~12 ppg, intervals of extremely weak rock could still be problematic.

Borehole stability during Phase 2 through the SAF

Phase-2 drilling and logging showed that the San Andreas Fault zone (a zone of damaged rock encompassing several currently active fault traces) extends from ~ 3180-3420m. The arkosic sandstones drilled through in the lower part of Phase-1 extend to a depth of 3160m. Below that depth, the formations encountered were mostly siltstones and claystones associated with the Great Valley formation. These rocks strike sub-parallel to the San Andreas Fault and mostly dip to the SW, such that the wellbore trajectory is roughly orthogonal to the bedding.[4]

The range of mud weights shown in **Fig. 14** were obtained from the analysis described above to achieve the desired degree of wellbore stability (breakouts that do not exceed 60° width) for the range of uncertainties in 's' illustrated in **Fig. 12**. As can be seen this results in a range of recommended mud weights between 10.2 and 12.2 ppg. The mud weights actually used during drilling are also shown in **Fig. 14**. As can be seen, the initial mud weight was 9.8 ppg and increased gradually with depth and was mostly within the range of mud weights indicated by the analysis described above.

Fig. 14 also shows the vertical and horizontal wellbore diameters as determined from acoustic caliper data obtained using logging while drilling (LWD). LWD data was obtained from 3050 to 3700m MD and a problem with the tool resulted in no data from 3550 to 3600m. Note that at depths above 3630m the hole is in good shape. The horizontal diameter is very close to the bit size and the vertical dimension shows only modest increases in hole size at a few depths. Hence, the mud weight predicted using the analysis above did a good job of maintaining wellbore stability during drilling most of the interval shown.

Another source of data that confirms this conclusion is the volume of mud in the hole as it was being drilled (**Fig. 15**). Hole volume is calculated assuming a cylindrical shaped borehole with variable diameter, defined by calipers with measured depth. Mud volume is estimated by correcting the hole volume for the volume of drilling assembly in the hole. Note that the actual mud volume is the same as that predicted for an in-gauge hole to ~3450m MD. However, the cumulative hole volume calculated from the LWD caliper data below 3450m show that the hole volume should have been essentially equivalent to that corresponding to an in-gauge hole to 3550m. This implies that the increase in hole volume seen in the interval between 3450-3550m MD was occurring higher up the hole as the acoustic caliper located only 14 m above the bit. Hence, there seems to be a degree of time-dependent failure of the hole at depths above 3450m while at the same time the hole was in gauge as it was being drilled from 3450-3550m. Time-dependent hole failure is discussed in more detail in the next section.

Between 3640m and 3700m MD, the acoustic caliper data (and hole volume data) show the onset of significant hole enlargements. In the acoustic caliper data, a moderate washout (approximately 2-3") is observed (**Fig. 14**). In the hole volume data (**Fig. 15**) we see an increase of volume with depth in excess of that expected if the hole was in gauge. Hence, we seem to be using a mud weight that is too low. One reason for this might be the fact that because the SAF was crossed at MD of ~3300m (TVD of ~2800m), the strength analysis described above (based on the sedimentary section drilled during Phase-1 to the southwest of the San Andreas Fault) might have resulted in an underestimate of the strength of the Great Valley formation on the NE side of the fault.

Time dependent failure

Once Phase-2 drilling was completed at a MD of 3980m, a six arm caliper log was run (**Fig. 16**). Surprisingly, this log showed very large hole enlargements, even in the interval from 3050-3650m where the LWD (and hole volume) data show that the hole was in gauge as it was being drilled. Thus, the enlarged calipers indicate deterioration of the borehole with time. Time dependent hole failure is clear for the depths covered by the LWD data as a direct comparison between **Fig. 15** and **Fig. 16**. The time dependent failure of the borehole was so severe that there are depth intervals where one (or two) of the calipers are fully extended. As shown in the inset of **Fig. 16** (a superposition of all the caliper data looking down the hole) the borehole seems to be primarily enlarged on the top of the hole. The blue symbols represent the tool position in the hole as determined using the algorithm described by Jarosinski[33]. The fact that the hole enlargements appear to be on the top of the hole might, in part, be an artifact of the

logging tool being near the bottom of the deviated well and the fact that the hole failure might have caused there to be a cuttings bed on the bottom of the hole.

One possible process responsible for the time dependent hole failure is that time dependent chemical reactions between the water based mud and the clays in shaly rocks decreased rock strength with time. However, the time dependent increase in hole size is seen over the entire depth range drilled in Phase-2, including the arkosic rocks extending to 3180m. Moreover, such interactions are not known to be a significant problem in the many oil and gas wells drilled with water based mud in the Great Valley formation in the region. The most likely possibility is time-dependent mud penetration into the rock surrounding the borehole. Fluid penetration around the well would increase pore pressure and reduce the effectiveness of mud weight to stabilize the hole and could cause cavitation of the rock surrounding the wellbore.

Fig. 17 shows LWD calipers and resistivity logs with multiple depths of investigation (tracks 1 and 2), and wireline calipers and resistivity logs which were measured after several days of LWD logs when drilling was completed (tracks 3 and 4). There is almost no separation in LWD resistivity logs but wireline resistivity logs from different depths of investigation are separated, indicating mud fluid penetration into the formation with time probably due to the numerous fractures in these formations. Below MD 3750m in **Fig. 17**, the post-drilling wireline caliper data indicate that hole is less enlarged which matches the minimal separation between the resistivity logs. This likely happened because of the low permeability of the formations and the fact that there was insufficient time for mud fluid to penetrate into the formation.

Modeling of time dependent failure

In this section we present a FEM (Finite Element Modeling) exercise to investigate mud penetration into the formation (and the change of pore pressure) surrounding the wellbore with time. Increase in the pore pressure promotes both failure of the intact rock as well as shear failure on fracture planes, both of which lead to enlargement of the borehole.

A FEM schematic model of the area surrounding the borehole is shown in **Fig. 18a**. We utilize realistic values for fracture permeability (~1mD) and matrix permeability (~0.004mD) for tight sandstones[34]. The borehole mud pressure of ~33MPa (used during drilling) and formation pore pressure of ~29MPa (estimated by in-situ measurements) are used as initial boundary conditions for the modeling.

Modeling of the pressure diffusion process indicates that mud starts penetrating the relatively high permeable fractures and gradually spreads out around the borehole with time. Hence, the initial shape of the diffusion front is dependent on the number of fractures and their intersecting locations with the borehole. The modeling shows the first sign of pressure change around the borehole at ~3hrs (**Fig. 19a**). **Fig. 19b**, **19c**, and **19d** show pressure changes after 2 days, 2 weeks, and 4 weeks, respectively. It illustrates that it takes 2-4 weeks for the pressure front to spread ~10-12 inches from the borehole wall, which is consistent with the rate of time dependent failure observed in the SAFOD borehole.

Incorporating the pressure changes shown in Fig. 19d into a three-dimensional model of potential wellbore failure, demonstrates that after ~4 weeks, on would expect a large zone of failure around the wellbore (reddish zone in **Fig. 18b**). For a symmetric distribution of fractures, the shape of the increased pore pressure area where fracture planes may slip is symmetric around the borehole. However, observed failures seem to be mostly on the top of the borehole (**Fig. 16** insert). Because of the high deviation angle of the well, removable blocks from the top section of hole fall into the hole but this would not happen for failing blocks adjacent to the bottom of the hole, thus leading to the appearance of asymmetric failure. The apparent asymmetry of the failure zone around the well is also enhanced by the accumulation of the failed material (a cuttings bed developed) on the bottom of hole.

Conclusions

This study defines a generalized workflow that could be applicable for wellbore stability analysis of wells located in areas with a complex stress field and little information about the rock strength. Using the predicted mud weights of ~10.5-12.5 ppg, the SAFOD borehole was successfully drilled through the SAF with relatively little failure (as indicated by LWD caliper and hole volume data). Six-arm caliper data collected after drilling showed significant increases in the size of the borehole with time, which is most likely caused by mud penetration around the well. Mud penetration is indicated by the separation in the resistivity logs (run with six-arm caliper) with multiple depths of investigation. FEM modeling shows that penetration of the drilling mud into the rocks surrounding the wellbore is a slow process which explains the time dependency on the wellbore stability. Once the pore pressure in these bedded and fractured rocks cross the threshold for shearing the fracture planes, failure occurs. Asymmetry in the shape of the failed wellbore is mostly coming from the fact that the SAFOD borehole is highly deviated (~54°), so failed blocks at the bottom of the borehole can not be removed. This effect is enhanced by accumulation of debris falling from the top and an artifact introduced by the tool lying at the bottom of the hole.

Acknowledgments

The SAFOD project is part of the EarthScope initiative of the U.S. National Science Foundation (NSF) that is being carried out in collaboration with the U.S. Geological Survey. Financial, engineering and technical help from the International Continental Drillling Program (ICDP) is gratefully acknowledged. The Stanford Rock and Borehole Geophysics consortium (SRB) funded PP during this project. We would like to acknowledge the scientists and engineers of the SAFOD team for their contribution to the success of the project. We thank GeoMechanics International (GMI) for use of its software in carrying out this study.

References

1. Chery, J., Zoback, M. D. and Hickman, S.: "A mechanical model of the San Andreas fault and SAFOD Pilot Hole stress measurements", Geophys. Res. Lett. (2004), 31.
2. Goodman, R. E.: "Introduction to Rock Mechanics", John Wiley and Sons (1989), 257-280.

3. Goodman, R. E., and Shi, G.: "Block theory and it's application to Rock Engineering", Printice-Hall Inc (1985).
4. Boness, N. and Zoback, M. D.: "A muiti-scale study of the mechanism controlling shear velocity anisotropy in the San Andreas Fault Observatory at Depth", Geophysics (2006), **71 (5)**, 131-146.
5. Zoback, M. D.: "SAFOD penetrates the San Andreas Fault", Scientific Drilling (2006), **2**, 32-33.
6. Sclumberger.: "Fullbore Formation MicroImager", FE_04_019_0, Product Marketing Communications, Houston (2004).
7. Zoback, M. D. et al.: "New evidence on the state of stress of the San Andreas fault system", Science (1987), **238**, 1105-1111.
8. Mount, V. S. and Suppe, J.: "State of stress near the San Andreas Fault: Implications for wrench tectonics", Geology (1987), **15**, 1143-1146.
9. Townend, J. and Zoback, M. D.: "Regional tectonic stress near the San Andreas fault in central and southern California", Geophys. Res. Lett. (2004), **31**.
10. Provost, A. S. and Houston, H.: "Stress orientations in northern and central California: Evidence for the evolution of frictional strength along the San Andreas plate boundary system", J. Geophys. Res. (2003), **108(B3)**, 2175.
11. Hickman, S. and Zoback, M. D.: "Stress orientations and magnitudes in the SAFOD Pilot Hole", Geophys. Res. Lett. (2004), **31**.
12. Brune, J. N., Henyey, T. L., and Roy, R.F.: "Heat flow, stress, and rate of slip along the San Andreas Fault, California", J. Geophys. Res. (1969), **74**, 3821-3827.
13. Lachenbruch, A. H. and Sass, J. H.: "Heat flow and energetics of the San Andreas Fault zone", J. Geophys. Res. (1980), **85**, 6185-6223.
14. Rice, J. R.: "Fault stress states, pore pressure distributions, and the weakness of the San Andreas Fault, in Fault Mechanics and Transport Properties of Rock", Academic (1992), San Diego, CA, 475-503.
15. Zoback, M. D., Hickman, S. and Ellsworth, W.: "The role of fault zone drilling in Earthquake Seismology - Treatise on Geophysics", ed. H. Kanamori and G. Schubert, Elsevier Ltd., Amsterdam (2007), **4**, 649-674.
16. Anderson, E. M.: "The dynamics of faulting and dyke formation with applications of Britain", Oliver and Boyd, Edinburg (1951).
17. Zoback, M. D.: "Reservoir Geomechanics", Cambridge University Press (2007), 84-137.
18. Peska, P. and Zoback, M. D.: "Compressive and tensile failure of inclined wellbores and determination of in situ stress and rock strength", J. Geophys. Res. (1995), **100(B7)**, 12791-12811.
19. Zoback, M. D., Barton, C., Brudy, M., Castillo, D., Finkbeiner, T., Grollimund, B., Moos, D., Peska, P., Ward, C., and Wiprut, D.: "Determination of stress orientation and magnitude in deep wells", J. Rock Mech. Min. Sci. Geomech. Abstr. (1998), **40**, 1049-1076.
20. Annor, A. and Jackson, R.: "Mechanical, thermal and joint properties of rock samples from the Lac du Bonnet Batholith, Manitoba: Geotechnical Studies at Whiteshell Research Area (RA-3)", CANMET Min. Res. Lab., Ottawa (1987).
21. Chang, C., Zoback, M. D. and Khakasar, A.: "Emperical relations between rock strength and physical properties of sedimentary rocks", J. of Petroleum Sc. and Engg. (2006), **51**, 223-237.
22. Moos, D. and Zoback, M. D.: "Feasibility study of the stability of openhole multilaterals, cook inlet, Alaska", SPE Mid-continent Operations Symposium, Oklahoma City, OK, SPE (1999).
23. Hoek, E. and Brown, E. T.: "Practical estimates of rock mass strength", Int. J. Rock Mech. Min. Sci. (1997) **34**, 1165-1186.
24. Hoek, E. and Brown, E. T.: "Empirical strength criterion for rock masses", J. Geotech. Engg. Div. (1980), **GT9**, 1013-1035.
25. Hongliang, H. and Ahrens, T. J.: "Mechanical properties of shock-damaged rocks", Int. J. Rock Mech. Min. Sci. & Geomech. Abstr. (1994), **31**, 525-533.
26. Hu, K. X. and Huang, Y.: "Estimation of the elastic properties of fractured rock masses", Int. J. Rock Mech. Min. Sci. & Geomech. Abstr. (1993), **30**, 381-394.
27. Jaeger, J. C.: "Behavior of closely jointed rock, Rock Mech. – Theory and Practice", Proceedings of the Eleventh Symposium on Rock Mechanics (1970), 57-68.
28. Chirkov, S. E., Popov, V. N., and Mirzoyan, A. A.: "Determination of the strength characteristics of jointed rocks in situ", J. of Mining Sc. (2006), **15**, 453-456.
29. Selby, M. J.: "A rock mass strength classification for geomorphic purposes with tests from Antarctica and New Zealand", Z. Geomorphology (1980), **24**, 31-51.
30. Thurber, C., Roecker, S., Zhang, H., Baher, S. and Ellsworth, W.: "Fine-scale structure of the San Andreas Fault zone and location of the SAFOD target earthquakes", Geophys. Res. Lett. (2004), **31**.
31. Moos, D., Peska, P., Finkbeiner, T., and Zoback, M. D.: "Comprehensive wellbore stability analysis using quantitative risk assessment", Jour. Petrol. Sci. and Eng., Spec. Issue on Wellbore Stability (2003), **38**, 97-109.
32. Ottesen, S., Zheng, R. H., and McCann, R. C.: "Wellbore stability assessment using quantitative risk analysis", SPE/IADC 52864 (1999).
33. Jarosinski, M.: "Contemporary stress field distortion I the Polish part of the western outer Carpathians and their basement", Tectonophysics (1998), **297**, 91-119.
34. Durrast, H., Rasolofosaon, P. N. J., and Siegesmund, S.: "P-wave velocity and permeability distributions of sandstones from a fractured tight gas reservoir", Geophysics (2002), **67**, 241-253.
35. Unsworth, M. and Bedrosian, P. A.: "Electrical resistivity structure at the SAFOD site from magnetotelluric exploration", Geophys. Res. Lett. (2004), **31**.

SI Metric Conversion Factors

bbl	x	1.589 873 E-01 = m^3
ft	x	3.048* E-01 = m
in	x	2.54* E-02 = m
ppg	x	2.245 322*E-02 = SG
psi	x	6.894 757 E-03 = MPa

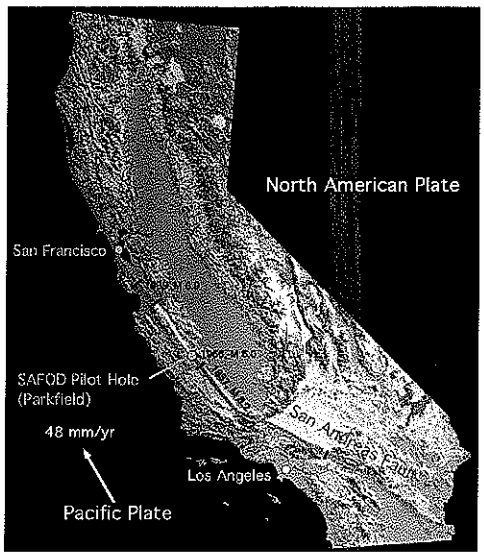

Fig. 1: The SAFOD borehole is located at Parkfield on a segment of the SAF that shows aseismic creep and repeating micro earthquakes. (Map from US Geological Survey)

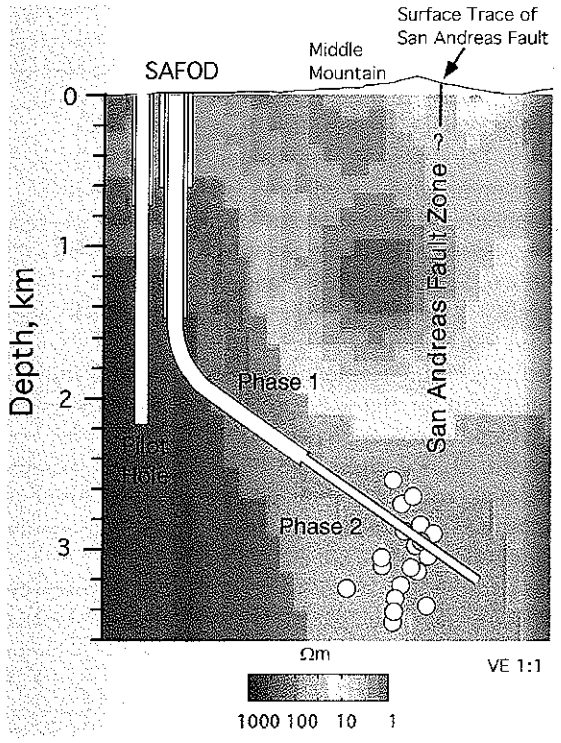

Fig. 2: A schematic of the SAFOD well trajectory superimposed on resistivity section determined from inversion of active source MT data[35].

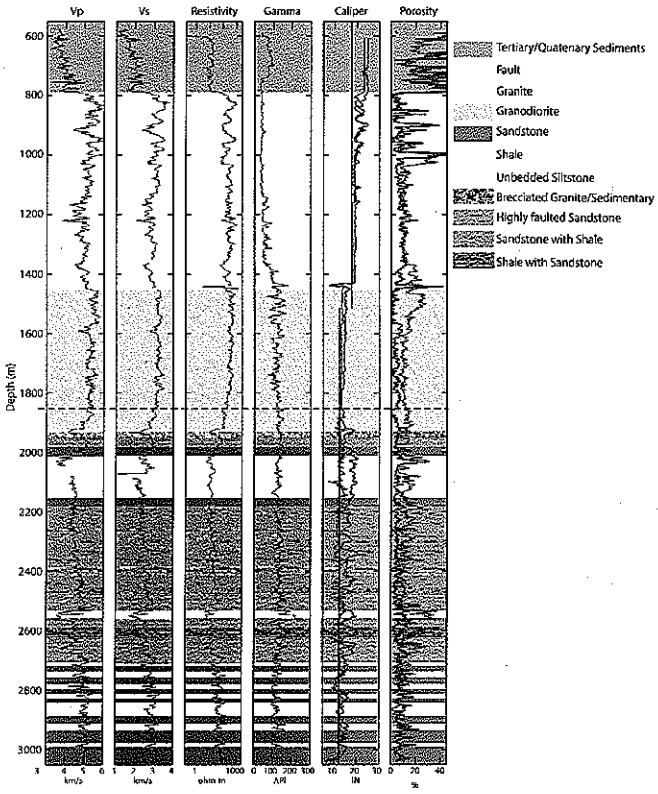

Fig. 3: A simplified lithology column calculated using petrophysical logs collected during the Phase-1 drilling of the SAFOD borehole.[5]

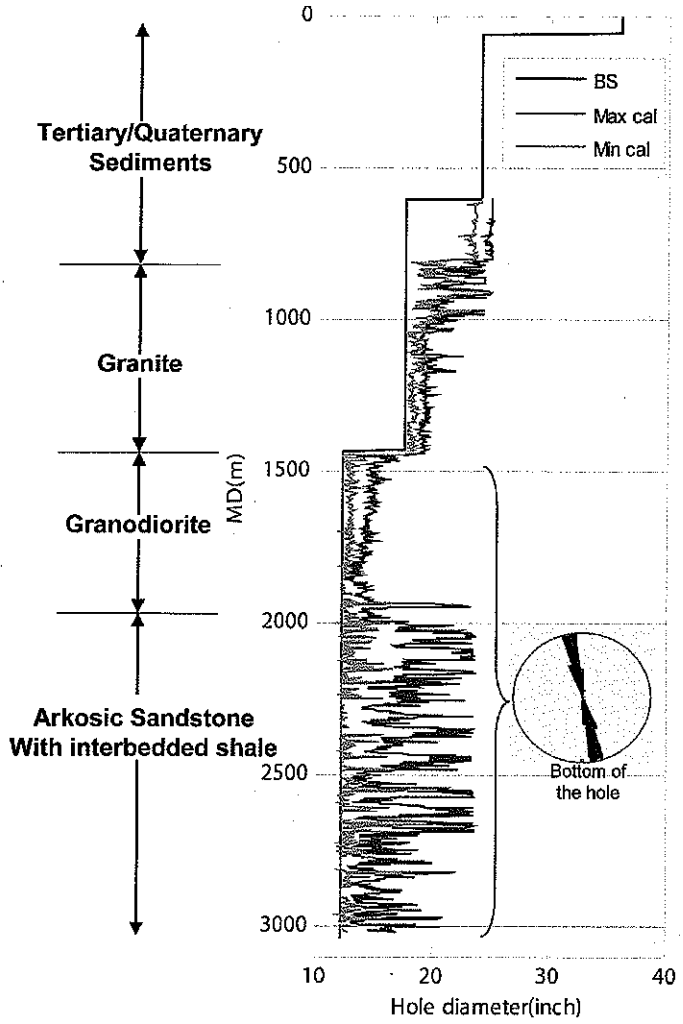

Fig. 4: Maximum and minimum caliper show borehole enlargements during Phase-1 drilling. Below 1440 m, borehole is elongated at ~10° anticlockwise tilt from the top of the hole.

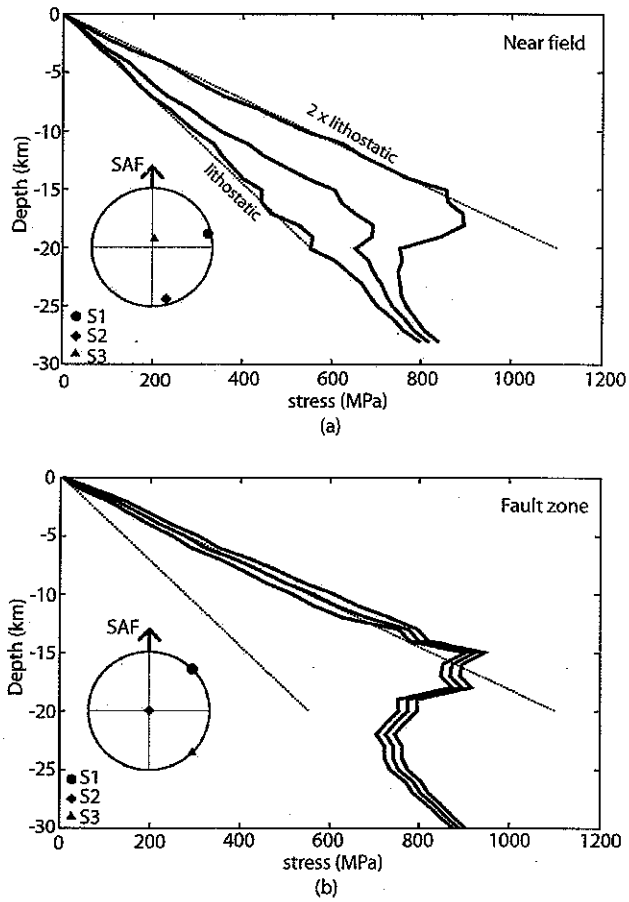

Fig. 5: S1, S2 and S3 profiles with depth and lower hemisphere stereo plots evaluated at 4km depth for (a) near field and (b) fault zone.[1]

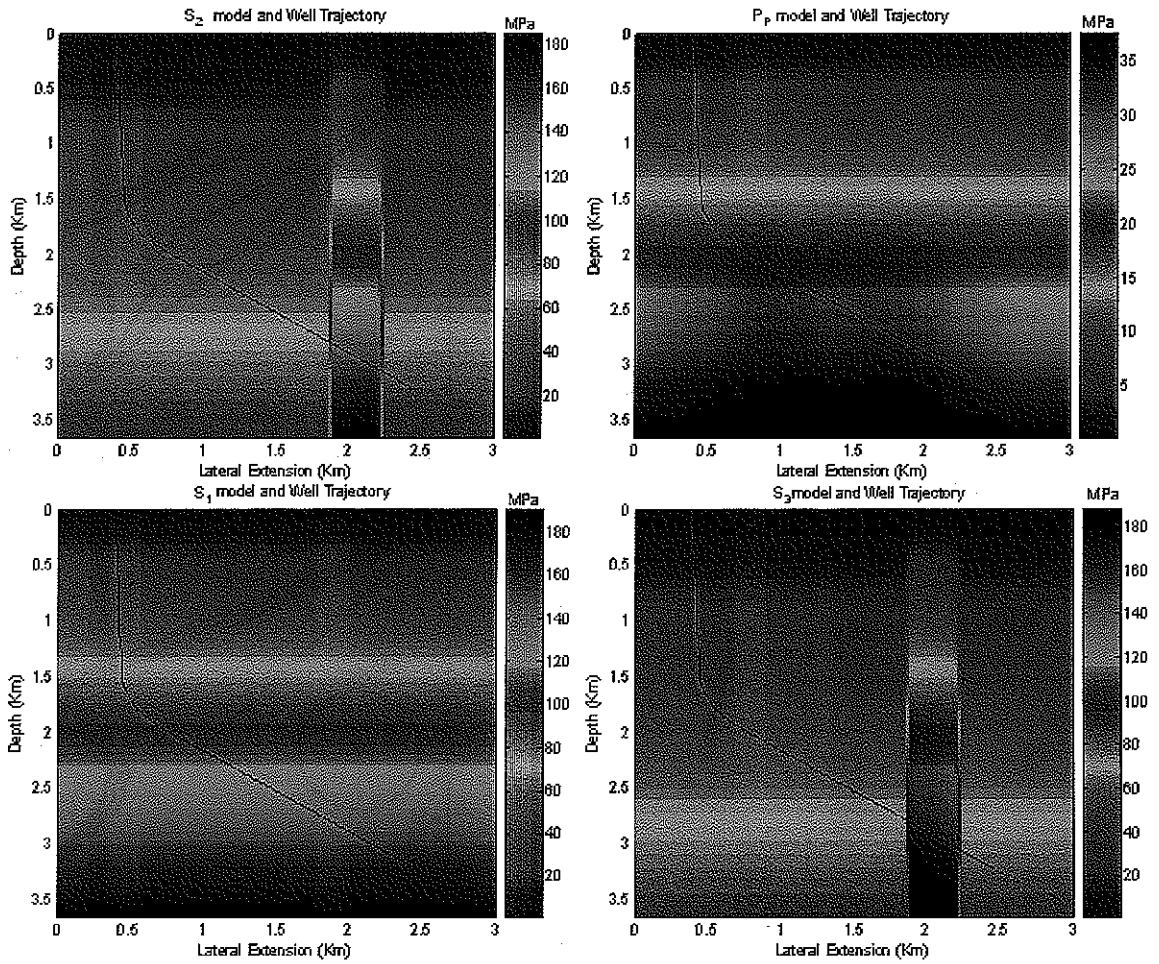

Fig. 6: Three principal stresses, S_1, S_2, S_3, and pore pressure, P_P, on the well trajectory plane. Black line shows the well path. The anomalous zone in S_2 and S_3 model at 1.8 km of lateral distance shows the San Andreas Fault zone.

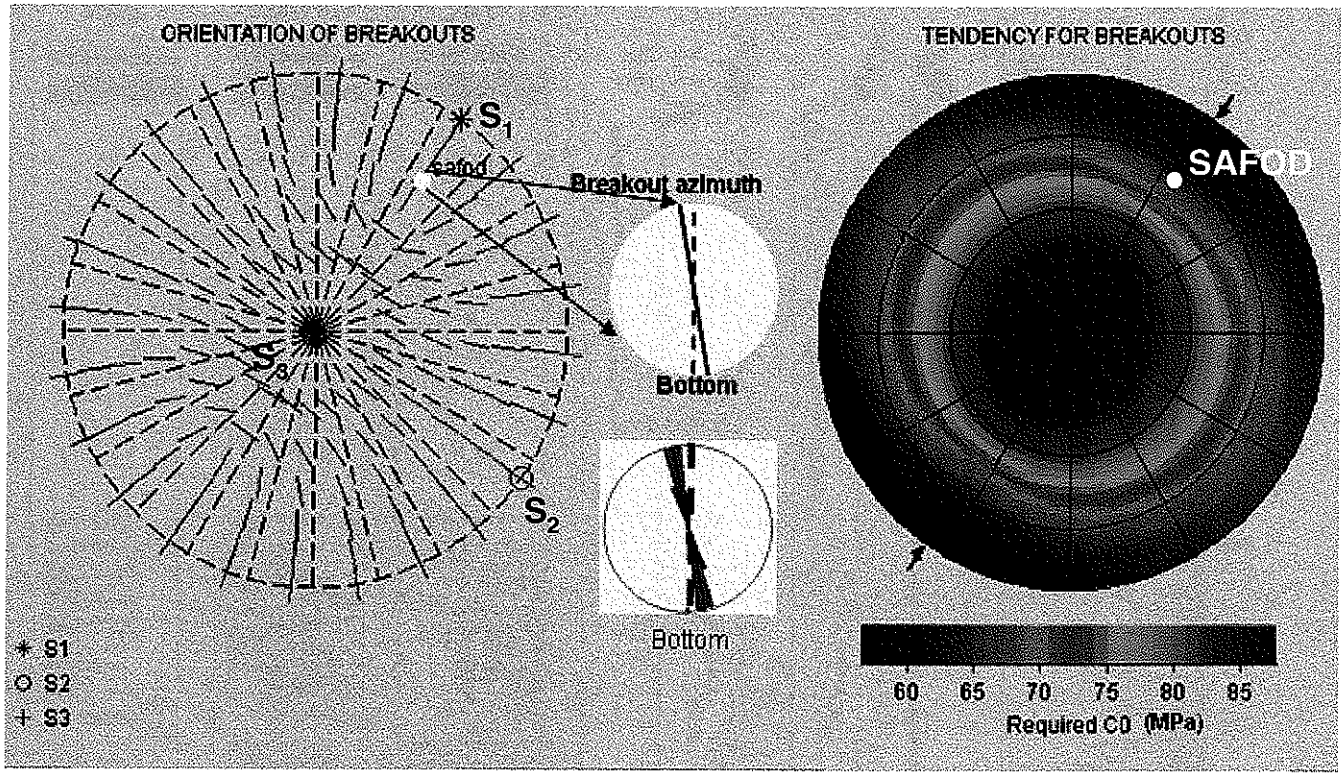

Fig. 7: Modified stress model with S_{Hmax} azimuth of 35 deg, $S_{Hmax} \approx 2*S_v$, $S_{hmin} \approx 1.82*S_v$, $S_v \approx$ lithostatic gradient (~0.025 MPa/m) is able to model breakout azimuth (blue), which matches the orientation of observed borehole enlargements (red).

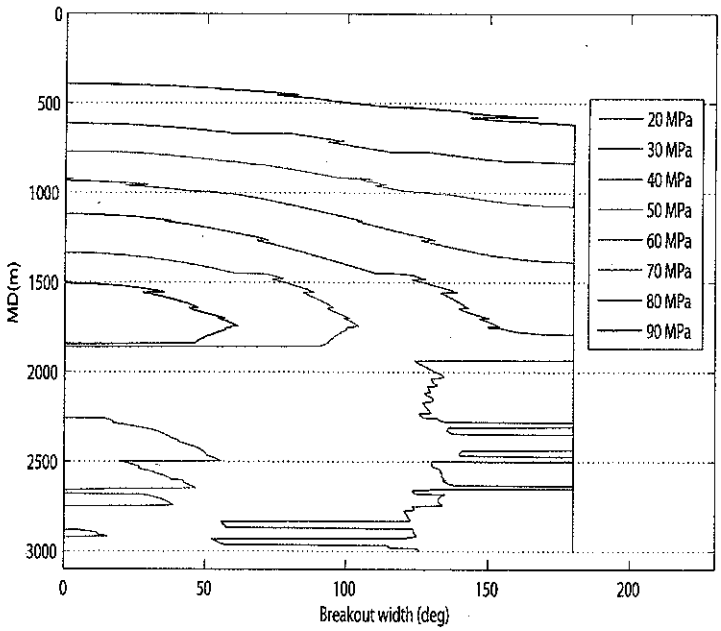

Fig. 8: At 1920m to 2804m (MD) of the SAFOD well trajectory, deterministic modeling indicates uniaxial compressive strength of ~ 60-70 MPa for a rock, which gives breakout width ~90° using mud weight of Phase-1 drilling.

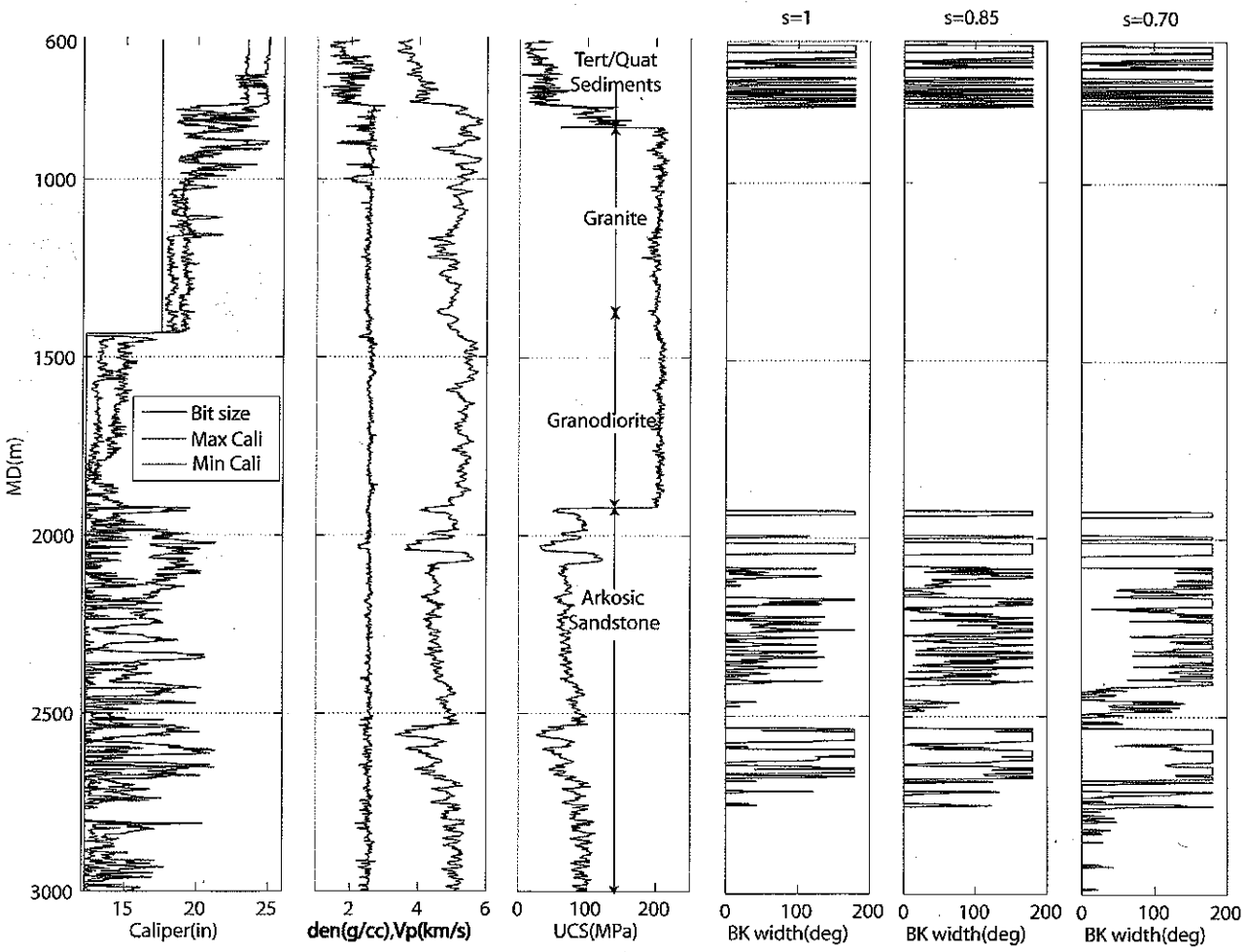

Fig. 9: Column 1: maximum and minimum calipers; column 2: density and P-wave velocity logs used for rock strength estimation; column 3: estimated uniaxial rock strength; column 4, 5, and 6: predicted breakout width with used mud weight using s=1, s=0.85, and s=0.7 in the sedimentary section below 1920m, and s=1 for granite, granodiorite, and tertiary sediments above 1920m.

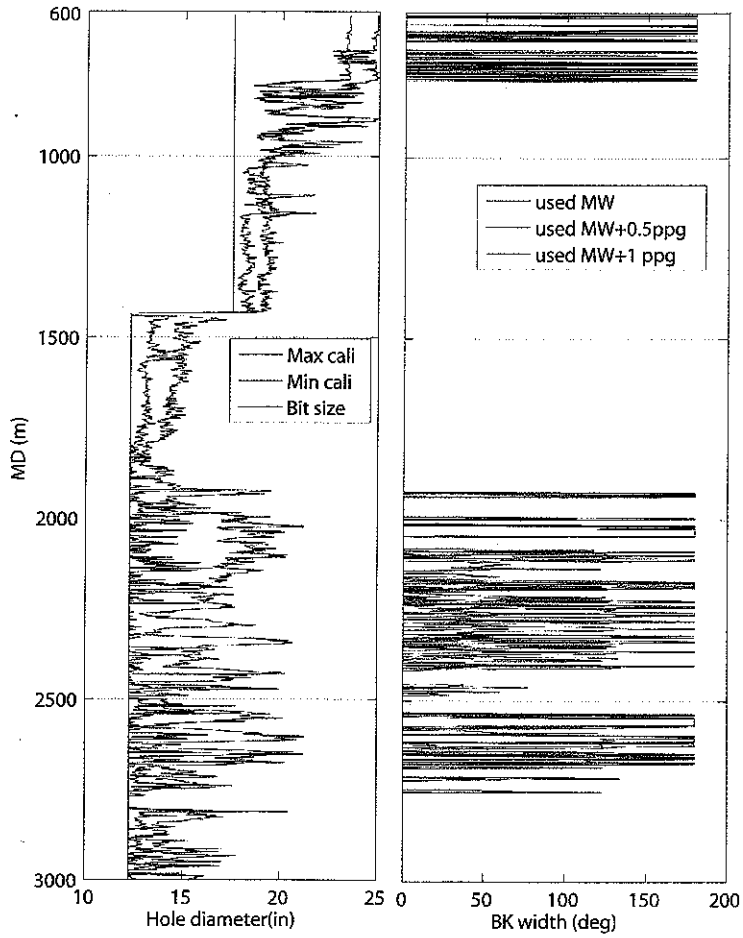

Fig. 10: Column 1: maximum and minimum calipers; column 2: predicted breakout width with rock strength (for s~0.85) for used mud-weight, and 0.5 ppg and 1 ppg higher mud-weights. An increase of ~1 ppg in mud-weight shows significant improvement in the borehole failure.

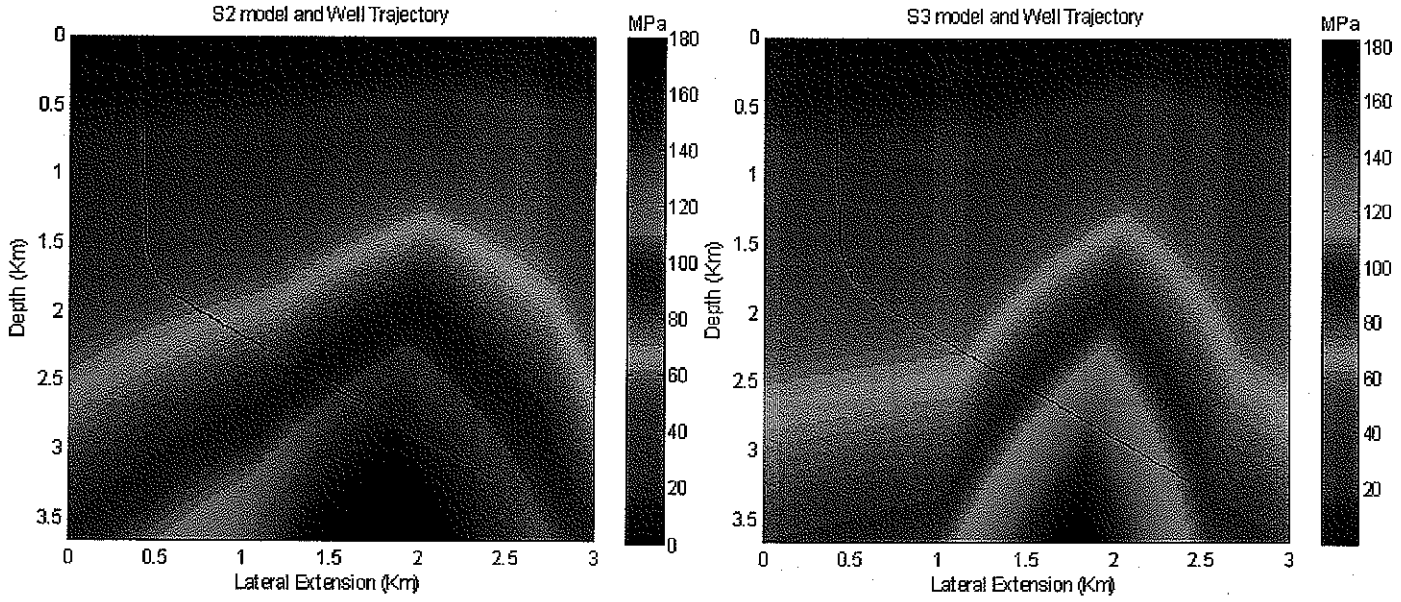

Fig. 11: Modified stress model for principal stresses, S_2 and S_3 through the San Andreas Fault. Pore pressure and S_1 remain same as Chery et al. model[1] (Fig. 6).

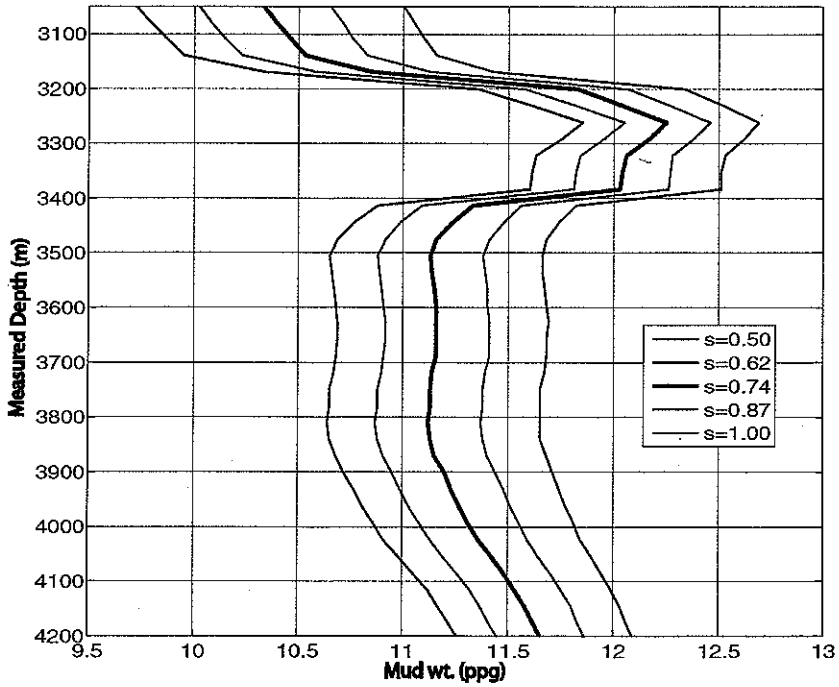

Fig. 12: Mud weight predictions using estimated rock strength and stress model for 60 deg breakout width. The analysis shows a minimum mud weight ~11.2 ppg (no damage, s=1) to 12.3 ppg (30% weaker than undamaged rock, s=0.5) is required to drill through the San Andreas Fault with a breakout width of ~60°.

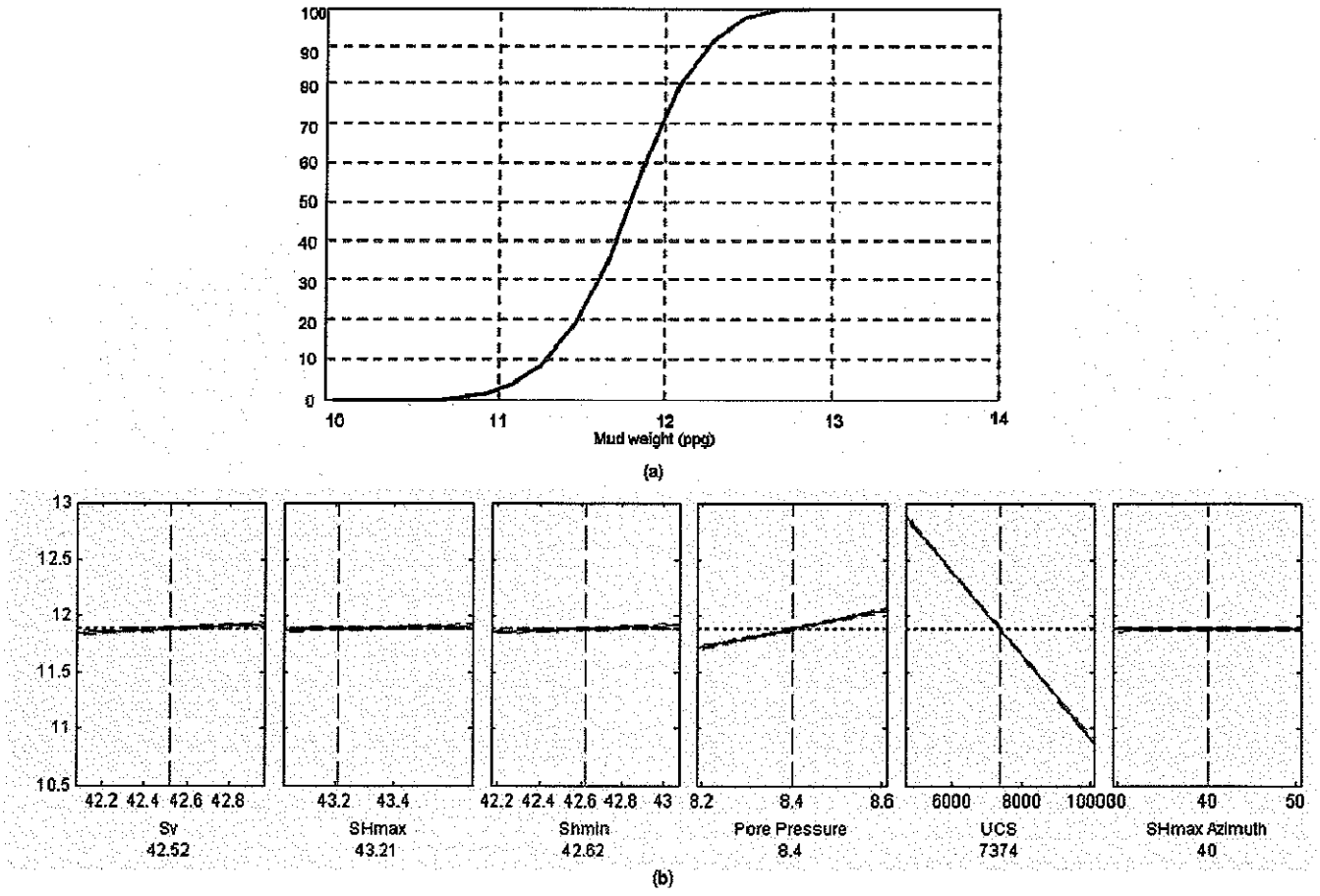

Fig. 13: (a) QRA at the San Andreas Fault zone (~3300m) the probability of success (to drill with 60° breakout width) as a function of mud weight. (b) The sensitivity analysis shows rock strength is the most sensitive parameter controlling the mud weight required to drill a stable hole through the fault zone. Stress and pore pressure are in ppg. UCS is in psi and S_{Hmax} azimuth is in degrees.

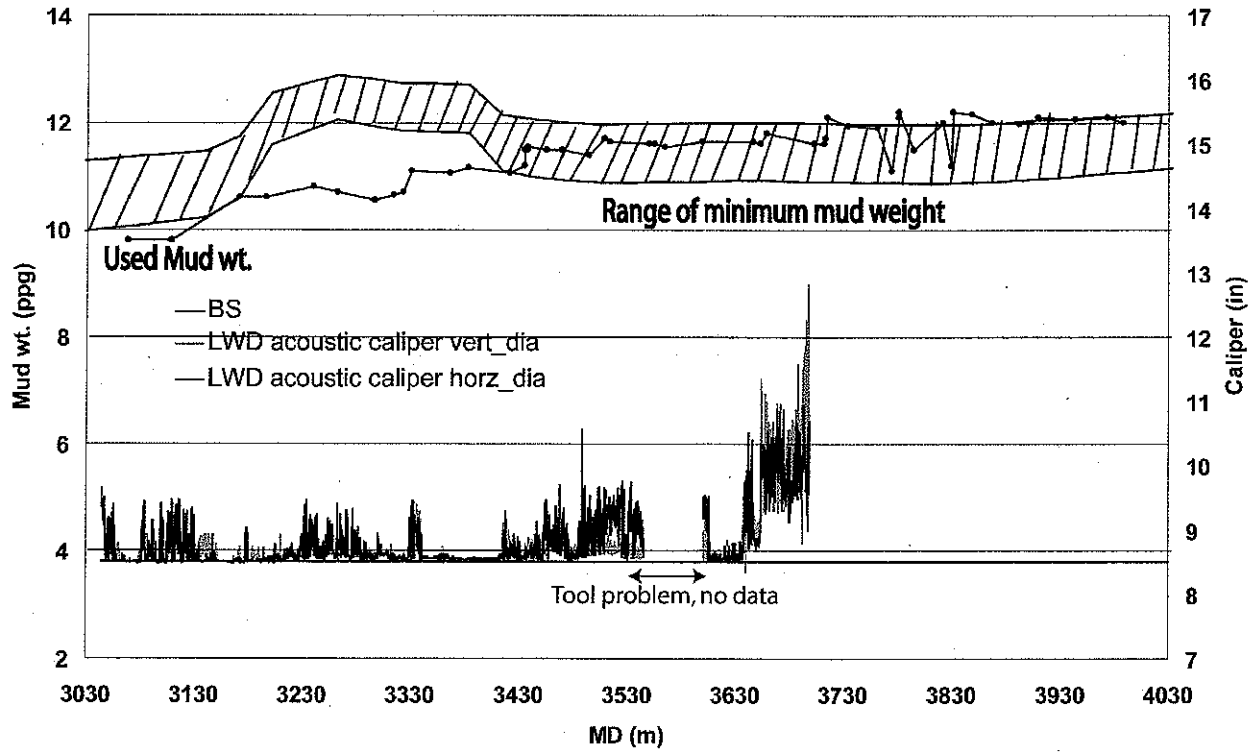

Fig. 14: Through the San Andreas Fault, LWD acoustic calipers show relatively little borehole failure in Phase-2 drilling when drilled with a mud weight close to predicted mud weight. Below 3650m, LWD shows onset of significant failure.

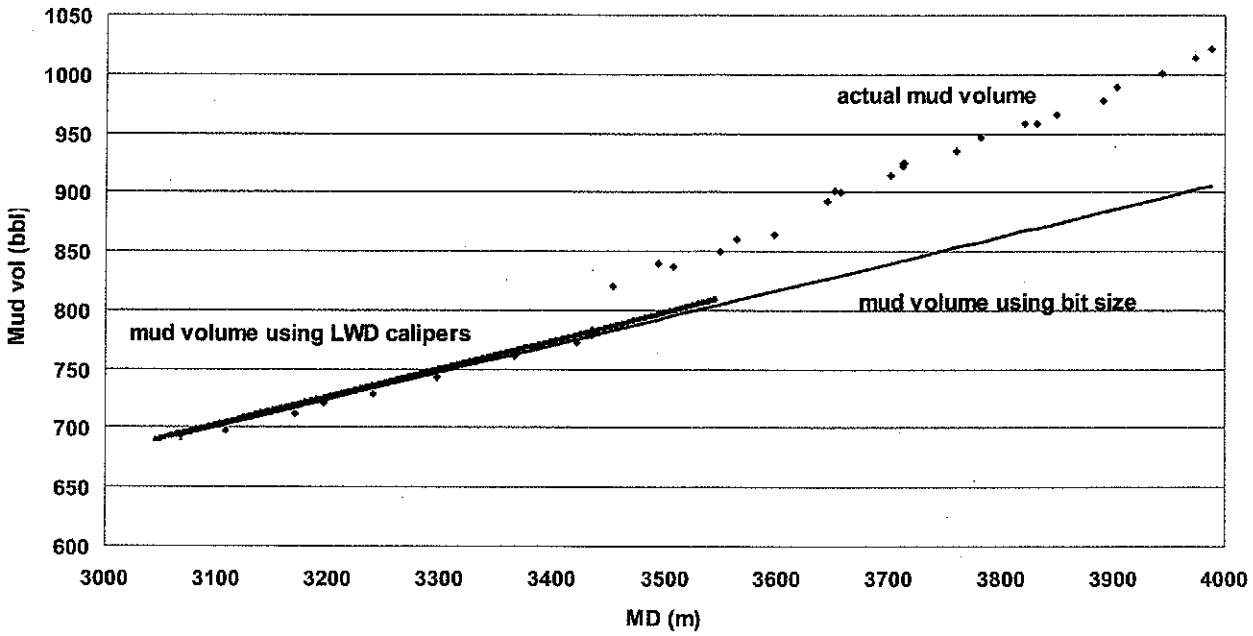

Fig. 15: A good match of the actual mud volume to mud volume estimates from the bit size and the LWD calipers indicates that the hole was relatively in good shape while drilling for the interval above 3440 m. LWD mud volume indicates good hole till 3550m (MD) while deviation of the actual mud volume from the bit size mud volume at this interval suggests a time dependent failures at interval above 3550m. Higher actual mud volume slope than bit size mud volume slope indicates onset of significant hole failure below 3550m.

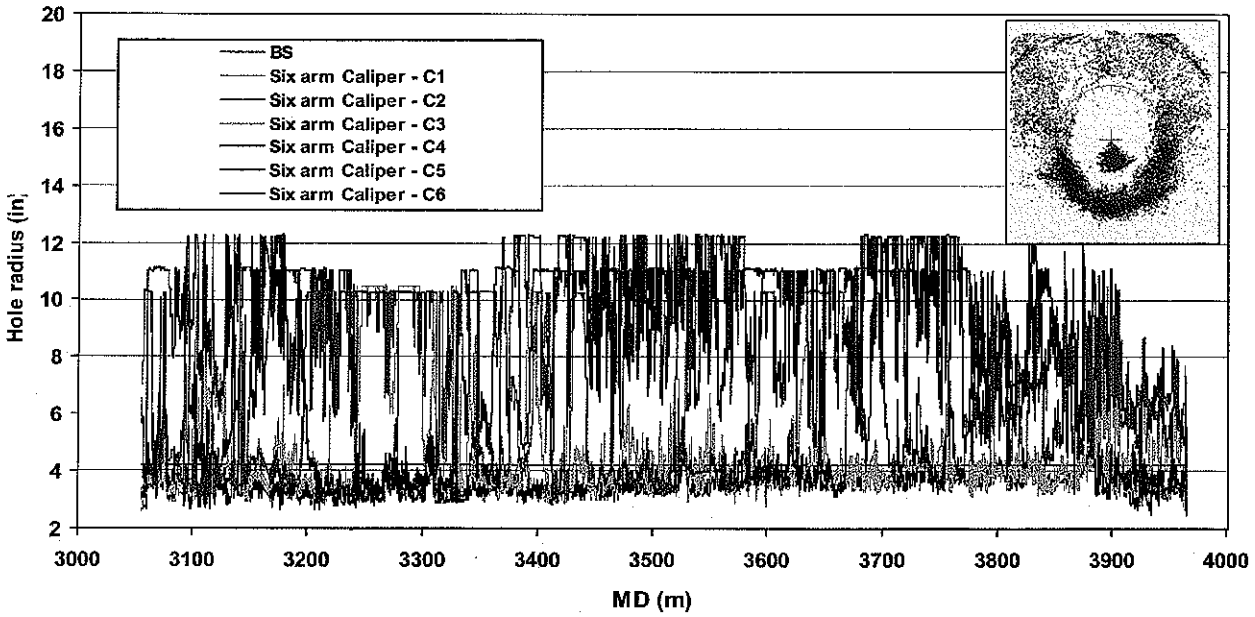

Fig. 16: Six arm wireline calipers show deterioration of the borehole with time. In the right up corner, centralized six-arm caliper pads are plotted in a borehole coordinate system. Borehole shape is highly extended at the top and top corners indicating failure in weak planes with time due to mud penetration.

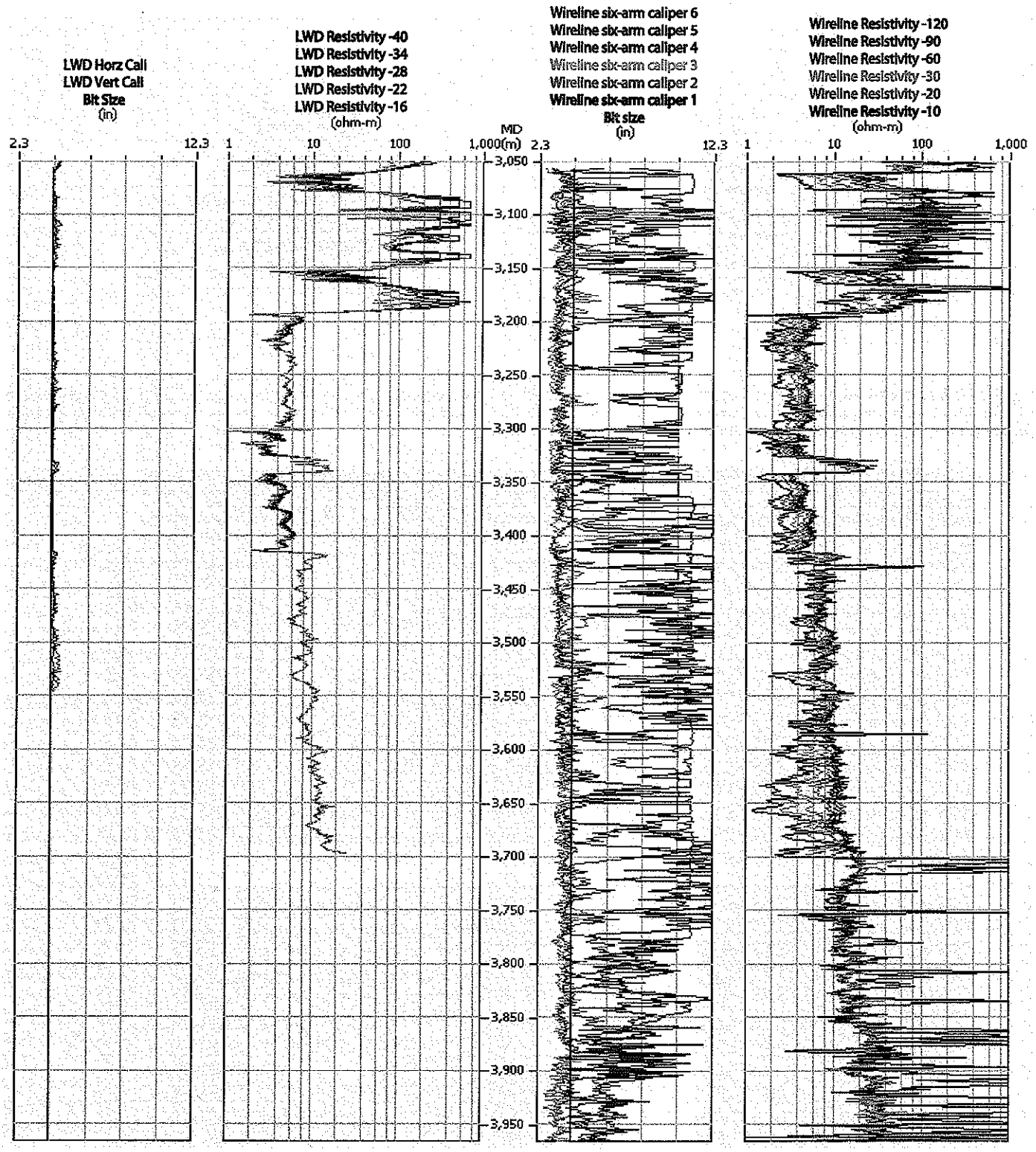

Fig. 17: LWD calipers (track 1) and resistivity logs with multiple depths of investigation (track 2) indicate a stable borehole and no fluid penetration around the borehole. Wireline resistivity logs (track 4) measured few days after the LWD logs show separation between them, indicating mud penetration into the formation which may cause failure in the borehole as observed by the wire line calipers (track 3).

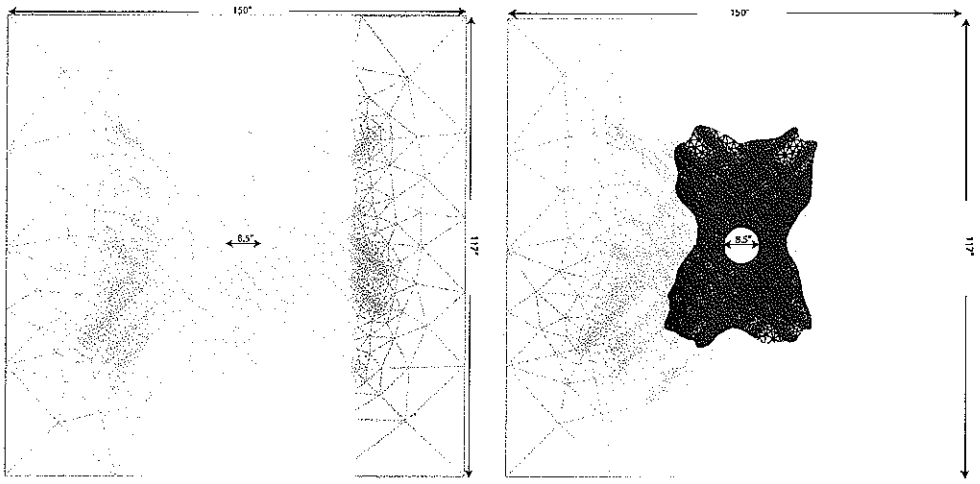

(a) (b)

Fig. 18: (a) A triangular mesh of the schematic model for the area around the borehole. Permeability values of 1mD and 0.004mD are used for fracture and matrix respectively. Mud pressure and pore pressure are kept at 33MPa and 29MPa respectively. (b) Red zone indicates zone of failure around the borehole due mud invasion

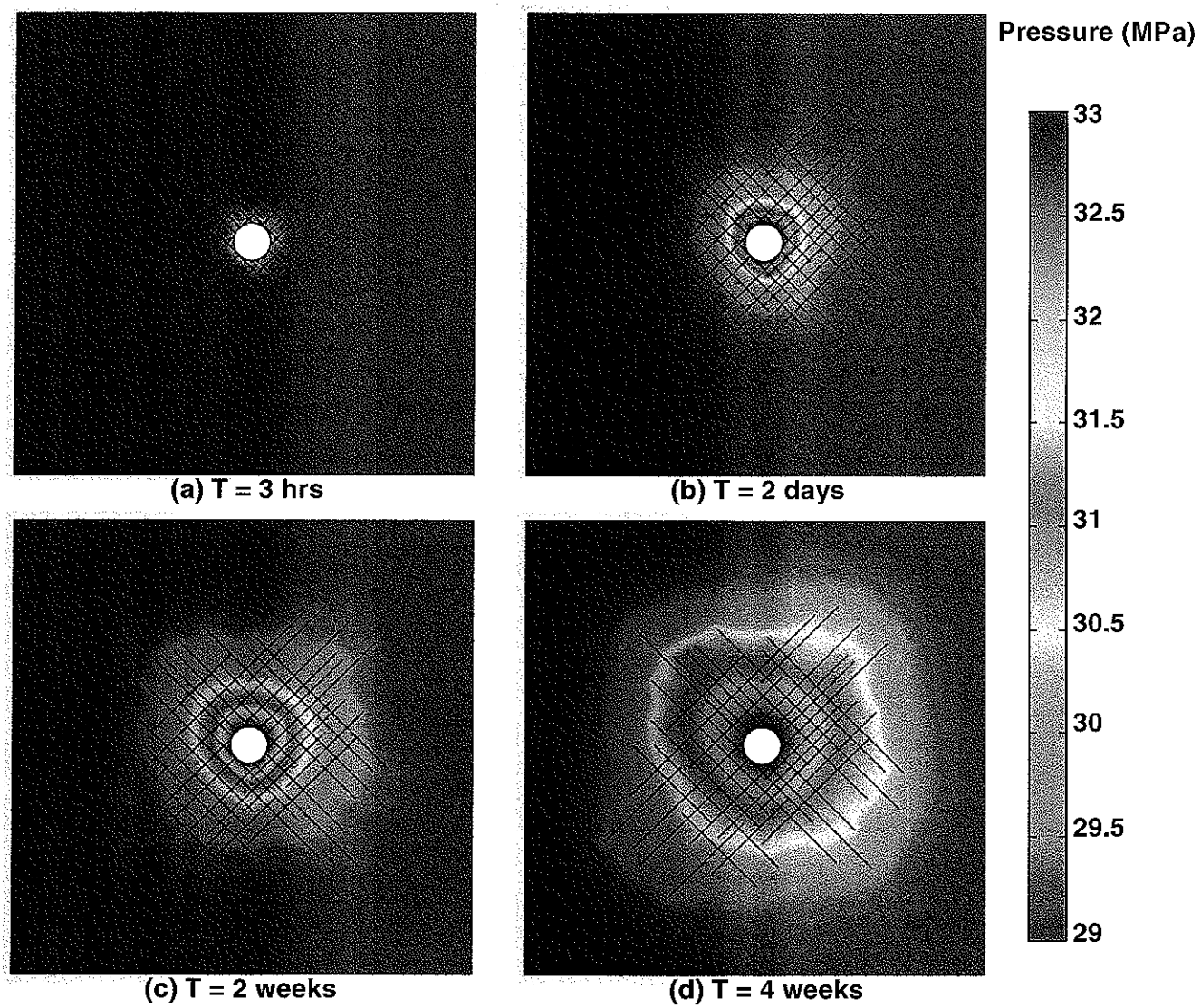

Fig. 19: Pressure front at (a) 3hours (b) 2 days (c) 2 weeks, and (d) 4 weeks show that it takes ~2-4 weeks for the front to spread up a mud wt. of ~33MPa to ~10-12 inches from the borehole wall by diffusion process (scale same as Fig. 18).